March 15, 2005

Crossover energetics for halogenated Si(100): Vacancy line defects, dimer vacancy lines, and atom vacancy lines

G. J. Xu, *University of Illinois at Urbana-Champaign*
Nikolai A. Zarkevich, *University of Illinois at Urbana-Champaign*
Abhishek Agrawal, *University of Illinois at Urbana-Champaign*
A. W. Signore, *University of Illinois at Urbana-Champaign*
B. R. Trenhaile, *University of Illinois at Urbana-Champaign*, et al.

Crossover energetics for halogenated Si(100): Vacancy line defects, dimer vacancy lines, and atom vacancy lines

G. J. Xu, N. A. Zarkevich, Abhishek Agrawal, A. W. Signor, B. R. Trenhaile, D. D. Johnson, and J. H. Weaver

Department of Materials Science and Engineering, Department of Physics, and Frederick Seitz Materials Research Laboratory,
University of Illinois at Urbana-Champaign, Urbana, Illinois 61801, USA

We investigated surface patterning of I-Si(100)-(2×1) both experimentally and theoretically. Using scanning tunneling microscopy, we first examined I destabilization of Si(100)-(2×1) at near saturation. Dimer vacancies formed on the terraces at 600 K, and they grew into lines that were perpendicular to the dimer rows, termed vacancy line defects. These patterns were distinctive from those induced by Cl and Br under similar conditions since the latter formed atom and dimer vacancy lines that were parallel to the dimer rows. Using first-principles density functional theory, we determined the steric repulsive interactions associated with iodine and showed how the observed defect patterns were related to these interactions. Concentration-dependent studies showed that the vacancy patterns were sensitive to the I concentration. Dimer and atom vacancy lines that were elongated along the dimer row direction were favored at lower coverage. Atom vacancy lines dominated at ~0.8 ML, they coexisted with dimer vacancy lines at ~0.6-0.7 ML, and dimer vacancy lines were exclusively observed below ~0.5 ML. These surface patterns reflect the mean strength of the adatom repulsive interactions.

PACS number(s): 68.37.Ef, 68.35.−p, 81.65.Cf, 31.15.Ar

I. INTRODUCTION

Recent studies of adsorbed Cl and Br on Si(100) demonstrated the surprising fact that these adatoms can destabilize the (2×1) surface and cause it to roughen.[1–6] This roughening occurs at temperatures far below those needed to cause desorption of volatile $SiX_2(X=Cl,Br)$.[1,3,5,7] Variable temperature scanning tunneling microscopy (STM) studies then revealed the dynamics of those changes as terrace vacancies formed and the released Si atoms produced islands on the terrace.[2–5,8] The underlying driving force for roughening can be traced in large measure to the repulsive interactions among the halogen atoms, and halogenated Si(100) is an ideal system for investigations of the effects of adsorbates on intrinsic surface energetics.[2,4,6,8]

Chlorine roughening is characterized by the production of dimer vacancy lines (DVLs) with the elongation of one-layer-deep pits along the dimer row direction, as depicted in Fig. 1(a).[3] Bromine roughening also leads to dimer vacancy lines but these dimer vacancy lines convert to atom vacancy lines (AVLs) that are separated by a dimer row when the Br concentration is high, Fig. 1(a).[5] Density functional theory (DFT) calculations for Br-Si(100) showed that atom vacancy lines allowed the Si-Br bonds to relax across the vacancies and relieve the strain.[9]

In this paper, we focus on the I-Si(100) system where we find surprises in surface patterns associated with adsorbate-induced roughening. Using variable temperature STM, we followed the evolution of I-saturated Si(100) at 600 K. In contrast to Cl and Br, we observed vacancies that elongated *across* dimer rows, denoted vacancy line defects (VLDs) and depicted in Fig. 1(a). We also carried out density functional theory calculations and derived the adsorbate-adsorbate repulsive interactions for I along and across the dimer rows. While the calculated steric repulsions favored defects along

dimer row directions for Cl and Br, the energies for I show a crossover that favored defect alignment across rows.

We then tuned the mean repulsive interactions by reducing the surface concentration. We found that vacancy line defects did not appear at intermediate coverage but that atom vacancy lines and dimer vacancy lines did. In turn, atom vacancy lines disappeared entirely below ~0.5 ML coverage. Thus, adsorbed iodine introduced a unique roughening pattern at high coverage, namely, vacancy line defects, but its effects were more similar to the smaller adatoms Cl and Br when the mean interaction strength was reduced.

II. EXPERIMENTAL CONSIDERATION

The experiments were carried out in an ultrahigh vacuum system (operating pressure $<5 \times 10^{-11}$ Torr) containing a variable temperature STM. The Si wafers were *p* type, B doped to 0.01-0.012 Ω cm, and oriented within 0.5° of (100) with miscut along [110]. Clean surfaces were prepared by degassing at 875 K for 12 h and then heating to 1475 K for 90 s at $<1 \times 10^{-10}$ Torr. Thermal treatments were done with resistive heating. An optical pyrometer was used to monitor the temperature during sample preparation, and the relationship between temperature and heating power was determined. During scanning, the temperature was adjusted by varying the heating power. The clean surface defect area was ~0.01-0.03 monolayer (ML), primarily in the form of dimer vacancies (DVs) and *C*-type defects.

A solid-state electrochemical cell derived from AgI doped with 7.5 wt. % CdI_2 provided a flux of I_2. Clean Si surfaces were exposed at room temperature to achieve the desired coverage. The adsorbate coverage was determined directly from the STM images where dimers that were terminated with iodine were readily differentiated from bare dimers (BDs).[5] The initially I-saturated samples were then imaged at
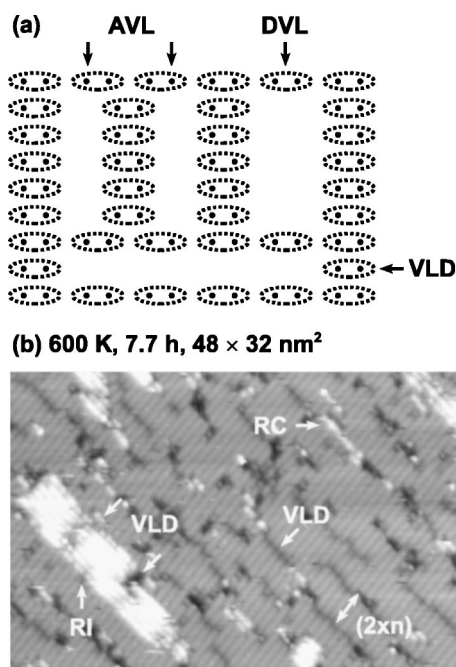
(a)   AVL   DVL

(b) 600 K, 7.7 h, 48 × 32 nm²

FIG. 1. (a) Schematic of Si(100)-(2 × 1) with two atom vacancy lines (AVLs) separated by a dimer row; a dimer vacancy line (DVL); and a vacancy line defect (VLD). I atoms are not shown. (b) Filled-state STM image (−1.7 V, 50 pA) of I-Si(100) taken after 7.7 h at 600 K. Dimer rows run from lower left to upper right. Bright features elongated perpendicular to this direction are Si regrowth chains (RCs) and regrowth islands (RIs). The dark features are dimer vacancies and vacancy line defects. These vacancy line defect structures are referred to as (2 × n) structures with n = 5-10. At this stage in surface evolution, the regrowth and vacancies account for ~6 and ~9 % of the surface.

600 K. In studies of surfaces with lower initial coverages, the samples were heated at 650 K for 30 min, cooled to room temperature, and then imaged. At elevated temperature, there was spontaneous iodine loss, as quantified by imaging before and after heat treatment, and the mechanism behind the loss of iodine will be discussed elsewhere.[10] Filled-state images were acquired with Pt/Ir tips in the constant current mode.

III. RESULTS AND DISCUSSION

A. Vacancy line defects: A new form of halogen roughening

Figure 1(b) reveals the surface morphology representative of I-Si(100)-(2 × 1) after 7.7 h at 600 K. Clearly visible in gray scale are the main terrace, where the dimer rows run from lower left to upper right, and grey irregular lines and bright features of various sizes that are elongated perpendicular to the terrace rows. Images taken at shorter times showed the gradual appearance of features like these as the surface roughened.

The grey features in the image represent dimer vacancies and vacancy line defects, as depicted in Fig. 1(a). They are one atomic unit lower than the terrace. Some segments of vacancy line defects are wider than one dimer (along the row), and they become darker. By 7.7 h, the vacancy line

defects extended across as many as ~10 dimer rows, and they started to form networks, with spacings between vacancy line defects along the dimer row direction that ranged from $4a$ to $9a(a = 3.84$ Å$)$. These structures are referred to as (2 × n) structures with n = 5 – 10. The bright features are one atomic unit higher than the terrace. They represent regrowth chains (regrowth features of one dimer width) and islands (at least two dimers in width) derived from Si atoms on the terrace. At 7.7 h, the regrowth and vacancies covered ~6 and ~9 % of the surface, respectively. The difference equals the initial defect density, indicating that there had been no loss of Si (no etching). Instead, Si atoms were transferred onto the terrace where they were able to form segments of a new layer, and this created terrace vacancies. This new mechanism, surface roughening without material removal, was recently proposed by Nakayama *et al.*[1] It was confirmed by Xu *et al.* in real time observations of surface evolution for Cl- and Br-Si(100) at 700 K.[3,5] Figure 1(b) also shows a large regrowth island (RI) that is roughened by two vacancy line defects that cut across it. Thus, roughening reactions similar to those on the terrace occur on islands as well.

Previous studies of halogens on Si(100) demonstrated that a key surface ingredient is a bare dimer because the reaction pathways that create vacancies require bare sites to which Si atoms can be transferred.[1,3,5] Thus, vacancy creation becomes more frequent as the concentration decreases from saturation. Here, the initial terrace coverage was 0.99 ML, and the concentration decreased gradually by desorption.[10] While iodine atoms were mobile at elevated temperature and could not be imaged, we can estimate the surface concentration during early-stage roughening from the density of vacancy line defects. Since there is no I within a vacancy line defect,[11,12] the vacancy line defect area minus the initial dimer vacancy density provides a lower limit to the amount lost, ~6% after 7.7 h.

The regrowth features in Fig. 1(b) are elongated perpendicular to the dimer row direction of the underlying terrace, bounded by long steps of S_A character and short steps of S_B character. The shape of two-dimensional islands is determined by both step free energies and surface strain energy.[8,13,14] Regrowth then follows the scheme observed previously in etching by hydrogen,[15] oxygen,[16] and halogens,[7] as well as during Si homoepitaxy.[17,18] Intriguingly, the image in Fig. 1(b) shows that the vacancy features do *not* follow the scheme observed previously in Cl- and Br-Si(100) systems, namely, dimer and atom vacancy lines, because the vacancy line defects are perpendicular to the dimer row direction.

B. Energetics of vacancy line defects

The novel vacancy features induced by I compared to Cl and Br can be understood by considering the energy change of a roughened surface. Herrmann *et al.*[2] recently argued that the change could be separated into contributions related to the creation of steps and changes in the steric repulsive interactions. The schematics in Fig. 2 show the relevant changes associated with the creation of an infinitely-long dimer vacancy line and vacancy line defect relative to a pris-
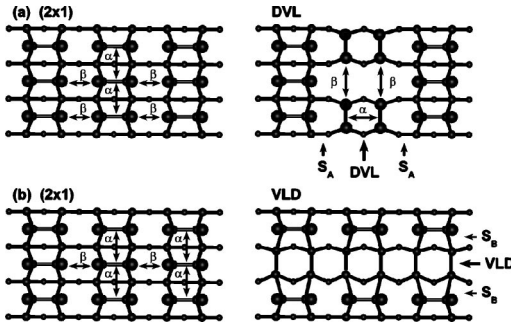
FIG. 2. (a) Schematic showing changes associated with creation of an infinitely-long dimer vacancy line relative to a pristine (2×1) surface. $\alpha(\beta)$ is the steric repulsive interaction for dimers in the same row (adjacent rows) and S_A and S_B are the step energies. The energy change for a unit of two dimers is $[2S_A + \alpha + 2\beta]$ $-[2\alpha + 4\beta] = 2S_A - \alpha - 2\beta$. (b) Changes associated with the creation of an infinitely-long vacancy line defect, where the energy difference is $[4S_B] - [4\alpha + 2\beta] = 4S_B - 4\alpha - 2\beta$.
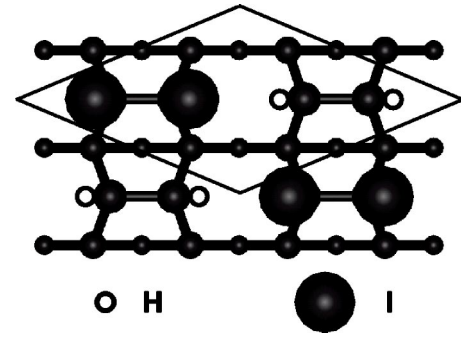

FIG. 3. Depiction of mixed hydrogen- and iodine-bonded Si(100)-$c(4 \times 2)$ where pairs of H and I alternate along and across the dimer rows. The values of α and β were negligible in this case. The rhombus shows the periodic boundary of the primitive cell.

tine surface. Specifically, the energy differences were compared in units of two dimers. The energies α and β are the intrarow and inter-row repulsive interactions, and S_A and S_B are the unit length step energies. In the dimer vacancy line structure, the exposed second layer atoms form dimers, and each Si atom is terminated with one I atom.[12] From the figure, the energy change is $[2S_A + \alpha + 2\beta] - [2\alpha + 4\beta] = 2S_A - \alpha$ -2β. In the vacancy line defect structure, the Si atoms of the exposed layer have one dangling bond but it is lost when a long Si dimer bond is formed and iodine chemisorption cannot occur. Hence, the change is $[4S_B] - [4\alpha + 2\beta] = 4S_B - 4\alpha$ -2β. Note that both processes cause the same number of Si atoms to be transferred onto the terrace.

According to our experimental results, the energy cost for a vacancy line defect must be lower than that for a dimer vacancy line, and this requires that $\alpha > (4S_B - 2S_A)/3$ for I. The energies for S_A and S_B steps have been determined from experiment to be 50 meV/$2a$ and 120 meV/$2a (a=3.84$ Å), respectively.[14] Hence, α is at least ~ 127 meV/$2a$.

To deduce the values for α and β for I-Si(100) from first-principles, we performed density functional theory calculations using the full-potential Vienna *ab initio* Simulation Package (VASP)[19–22] with ultrasoft pseudopotentials.[23,24] The energies of the surface were calculated for three configurations, namely, with H termination of the Si dangling bonds, with I termination of those bonds, and with alternating H and I (pairwise) termination along and across the dimer rows, Fig. 3. The hydrogen-terminated state provides a reference to calculate the steric repulsive interactions as it has the same symmetry with no Si dangling bonds. The calculations were performed for a slab of seven Si layers that was repeated as a periodic array with an interslab spacing of at least 15.9 Å. The unit cell (rhombus) shown in Fig. 3 contains 40 atoms. The bottom two layers were fixed at the Si bulk lattice position and were terminated with H. All other atoms were fully relaxed until the atomic forces were less than 0.03 eV/Å. In all three cases, we used the same unit cell shape, the same Monchorst-Pack[25] k-point mesh ($4 \times 4 \times 4$ k points per unit cell), and the same energy cutoff (349.46 eV) of the plane

wave basis so that systematic errors in energy differences would cancel. Increasing the number of k points, the energy cutoff, the number of layers, or the slab separation did not alter the calculated relative energies. The estimated relative energy error is less than 10 meV per unit cell. Reducing the number of layers to six led to different relaxations of the surface atoms but no significant changes in the calculated relative energies, whereas the results for a five-layer slab had not converged sufficiently.

Figure 3 illustrates the mixed H-I configuration where pairs of H and I bond to every other Si dimer along and across the dimer row. In this case, the interactions α and β are not present, compared to the all-I termination. We also assumed that $\alpha \approx 2\beta$, an approximation that is reasonable given the previous calculations for F, Cl, and Br (α arises from the interactions of four halogen atoms while β is caused by two).[2] From the calculations, we deduced α $=150\pm10$ and $\beta=75\pm5$ meV/dimer for I. The calculated intrarow repulsion α is then in good agreement with the estimate based on experiment. Herrmann *et al.*[2] reported values of 61 and 26 meV for Cl and 106 and 52 meV for Br.

From the calculations, the energy associated with dimer vacancy line creation for a unit of two dimers is −200 meV and that with vacancy line defect creation is −200 meV, where the negative sign indicates a lowering of surface energy in both cases. Clearly, vacancy line defects are favored over dimer vacancy lines, as observed experimentally.[3,26] The corresponding values for Cl and Br are given in Table I, and they are in agreement with experiments that show defect elongation along the rows. Moreover, the trend from Cl to Br to I indicates that halogen species with larger atomic size cause greater destabilization of the surface.

Inspection of the vacancy line defects of Fig. 1(b) shows that they exhibit kinks that are not included in Fig. 1(a). In contrast, dimer vacancy lines, which were previously observed in Cl- and Br-Si(100) (Refs. 1–3 and 5) or for I-Si(100) at lower coverages (discussed below), rarely have kinks. This reflects the fact that the energy to create a kink in an S_A step is much higher than that needed to create one in an S_B step (the kink creates a unit of S_B character in an S_A step but S_A character in the S_B step). At elevated temperature, steps on clean Si undergo fluctuations determined by those energies, and the population of kinks reflects the Boltzmann

TABLE I. Energy changes (in units of two dimers) associated with the creation of the infinitely long dimer vacancy lines and vacancy line defects of Fig. 2 for Cl, Br, and I. For I-Si(100), the vacancy line defect structure is favored. For Cl- and Br-Si(100), dimer vacancy lines have the lower energy.

	DVL $2S_A - \alpha - 2\beta$ (meV)	VLD $4S_B - 4\alpha - 2\beta$ (meV)
Cl	−13	184
Br	−110	−48
I	−200	−270

factor at that temperature. The presence of I alters the energies, but not the relative magnitudes, as was shown for Cl-Si(100).[8]

It is important to note that the vacancy line defects reported here are thermodynamically favored for a surface with high I concentration and bond strain. These vacancy line defects are analogous to those observed on Ge-covered Si(100), where the larger lattice constant of Ge led to compressive strain (i.e., repulsive interactions).[27,28] Their effect is the opposite of vacancy line defects produced by ion sputtering,[29,30] etching,[7,15,16] or metal contamination[31] where the surface energy is raised relative to the pristine state.[31–33] Zandvliet and co-workers[31,34] showed that randomly created vacancies would favor alignment perpendicular to rows for vacancy concentrations <0.2 ML because there is an attractive interaction between vacancies in adjacent rows and a long-range repulsive interaction between vacancies within the same rows.[31,35–37] At higher vacancy concentrations, dimer vacancy lines with length greater than three dimers are favored over vacancy line defects.[38]

C. Surface patterns and their dependence on coverage

The analysis above indicates that a necessary condition for vacancy line defect formation or I-Si(100)-(2×1) is that $\alpha > (4S_B - 2S_A)/3 \approx 127$ meV/$2a$. To determine whether we could tune the repulsive interactions, we reduced the surface concentration, expecting interactions to decrease in a mean-field sense. If that were the case, we reasoned that it might be possible to pass out of the regime where vacancy line defects were favored, and the patterns would resemble those observed for the halogens with lower steric repulsive interactions, namely, atom vacancy lines or dimer vacancy lines. For these studies, we exposed the sample at room temperature to obtain the desired coverage, imaged at room temperature to determine the coverage, heated to 650 K for 30 min, and then imaged again at room temperature.

Figure 4(a) shows a surface with an initial coverage of ∼0.9 ML, after a thermal cycle that resulted in a final coverage of ∼0.8 ML. The dimer rows run from lower left to upper right. The bright features are again regrowth structures.[1,3,5] They appear primarily as regrowth chains (RCs) of one to seven dimers. Most are derived from an odd number, and we believe that the end dimers rebond to sub-
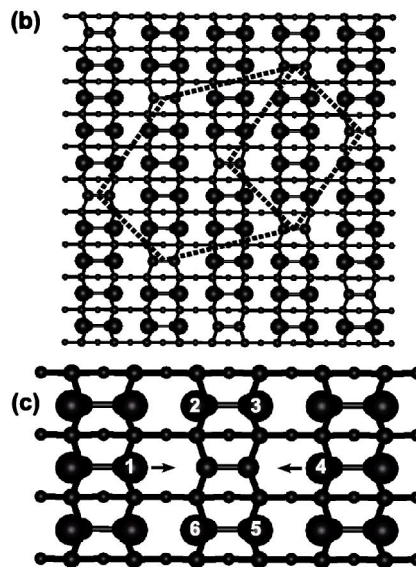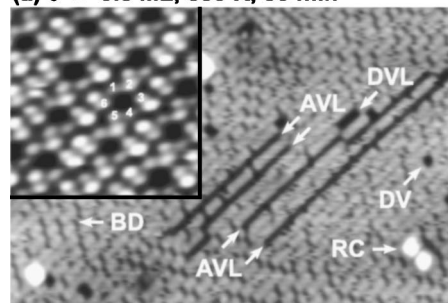

FIG. 4. (a) Filled-state image (−2 V, 120 pA) taken at room temperature (30×20 nm²). The initial I concentration was ∼0.9 ML and the final was ∼0.8 ML. Dimer rows run from lower left to upper right. The bright features reflect adatoms of Si on the terrace in the form of regrowth chains (RCs). The dark gray features are bare dimers (BDs), and the isolated black features that are lower in density are dimer vacancies (DVs). Atom vacancy lines are indicated, together with dimer vacancy lines that were occasionally observed. The inset (4.5×4.5 nm²) is an atomic resolution empty-state image (+1.7 V, 50 pA) that shows the chemisorption structure of I at 0.8 ML. The dark holes are bare dimers and the smaller, bright features are individual I adatoms. (b) Schematic of the 0.8 ML chemisorption geometry of I, where six bare dimers that are connected by dashed lines around a central bare dimer exhibit pseudo-six-fold symmetry. The smaller parallelogram represents the unit cell of this $p(2\sqrt{2} \times \sqrt{13})R56.3°$ structure. (c) Schematic showing the relaxation and bond angle rotation of six neighboring I adatoms around a central bare dimer. Atoms 1 and 4 have relaxed 1.9±0.3 Å toward the bare dimer.

strate dimers, as observed at low coverage for Si homoepitaxy on Si(100).[39] Iodine-free sites are required when Si adatoms meet with partners to form regrowth features, and the situation is analogous to that on the clean surface.[1,3,5] Regrowth islands that are two rows in width were occasionally observed. Bare dimers appear as gray features of one dimer size (better seen in images at lower coverage). They can be distinguished from single dimer vacancies (DVs) because the latter are much lower in density and are darker. Statistical analyses over several images (75×75 nm²) showed that Si

regrowth and vacancy features covered ~1.6% and ~2.6% of the surface, respectively. The difference is close to the initial defect density of this surface, implying the conservation of Si atoms on the surface at 650 K.

As demonstrated by Fig. 4(a), the reduction of I results in surface destabilization that favors dimer vacancy lines and atom vacancy lines structures rather than vacancy line defects. This reflects a reduced mean adsorbate-adsorbate repulsive interaction. Four atom vacancy lines are marked in Fig. 4(a), together with a dimer vacancy line derived from five dimer vacancies. The surface area covered by atom vacancy lines was ~20 times that of dimer vacancy lines (single dimer vacancies were not counted). The atom vacancy line pair at the left is separated by a single dimer row, establishing a local (3×2) symmetry. It is connected to a region where two dimer rows separate the vacancy lines in a (5×2) symmetry. The pair at the right also has (5×2) symmetry and connects to a region with (3×2) symmetry.[3] Some atom vacancy lines were as many as 50 dimers in length (not shown).

The chemisorption geometry of I at 0.8 ML is best illustrated in the inset of Fig. 4(a). [The main image of Fig. 4(a) is a filled-state image and there is a deep minimum between the dimer rows; in the inset, the minimum appears along the center of the rows since it is an empty-state image.] Dimer rows run from bottom left to upper right, as in the main image. The dark features represent I-free dimers while the smaller bright features are individual iodine atoms bonded to terrace atoms. The distribution of bare dimers and I-terminated dimers is shown schematically in Fig. 4(b) where six bare dimers connected by dashed lines around a central one define a pseudo-six-fold symmetry. The dashed parallelogram represents the unit cell of this $p(2\sqrt{2} \times \sqrt{13})R56.3°$ structure.

It is important to note that the I atoms in the inset do not all have the same contrast. The six neighboring adatoms around a bare dimer, enumerated in the inset of Fig. 4(a), appear darker than the others. Their structure is depicted schematically in Fig. 4(c). Analysis of the position of atoms 1 and 4 indicates that each has relaxed 1.9±0.3 Å toward the central bare dimer. This is reasonable since bare dimers provide extra space and bond angle rotation reduces the steric repulsive interactions. Indeed, de Wijs and Selloni[9] have reported that the Br-Br (Cl-Cl) intra-dimer distance increased from 3.87 (3.84) Å in the (2×1) reconstruction to 3.99 (3.88) Å in the (3×2) reconstruction, because the steric constraints of the former were lessoned in the latter [see schematic in Fig. 1(a)].

Figure 5(a) shows a surface that had an initial coverage of ~0.7 and a final coverage of ~0.6 ML. Inspection reveals two chemisorption phases. In one, alternate dimers are I-free, producing a $c(4 \times 2)$ structure with 0.5 ML (discussed further below). In the second, every third dimer is bare, corresponding to a $p(6 \times 3)$ structure with 2/3 ML coverage, as in Fig. 5(b). Regrowth and vacancies account for ~3.7 and ~4.6 % of the terrace area, respectively, with some vacancies having coalesced to form pits, as in the lower right of Fig. 5(a). The regrowth features are now longer, with some reaching 30 dimers. Regrowth islands that were two dimers
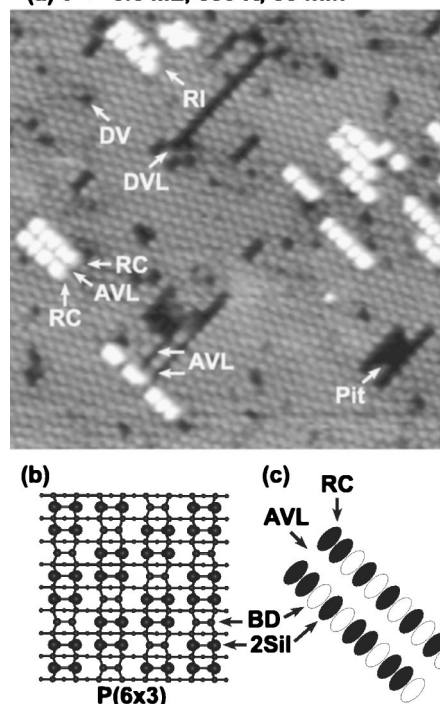

(a) θ ≈ 0.6 ML, 650 K, 30 min

(b)   P(6x3)   **(c)**   RC   AVL   BD   2SiI

FIG. 5. (a) Filled-state image $(-2 \text{ V}, 120 \text{ pA})$ of a surface with initial and final coverages ~0.7 and ~0.6 ML$(30 \times 30 \text{ nm}^2)$. Regrowth islands (RIs) were frequently two dimers in width. Vacancies coalesced to form pits, such as the one at lower right. Two chemisorption structures were present. The $p(6 \times 3)$ structure corresponds to 2/3 ML coverage where every third dimer is bare, as illustrated in (b). The $c(4 \times 2)$ corresponds to 0.5 ML. (c) illustrates the regrowth chains at lower left of (a) where they are separated by an atom vacancy line. On it, the distribution of I atoms is depicted.

wide were frequently observed. At ~0.6 ML, however, the steric repulsive interactions are still significant and many of the regrowth chains are separated by one atomic vacancy line. The structure of the regrowth chains at left center is illustrated in Fig. 5(c), including the distribution of iodine on the chains. Given the repulsive interaction α, I occupation by alternate dimers is favored. The presence of the atom vacancy line minimizes the importance of β.

Xu et al.[3,5] reported that atom vacancy lines were formed by splitting existing dimer vacancy lines for Cl- and Br-Si(100), and that they could convert back to dimer vacancy lines, depending on the local halogen concentration (energy balance). de Wijs and Selloni[9] calculated that the atom vacancy line structure is energetically favored at high coverage for Br-Si(100) because of the Br-Br steric repulsive interactions. An atom vacancy line pair of length n allows relaxation for $4n$ adatoms whereas one dimer vacancy line allows relaxation of only $2n$ adatoms. They also calculated the energies at 2/3 ML and found that dimer vacancy lines were favored over atom vacancy lines. This is because the stress induced by the phase shift between (3×2) and (2×1) regions was now significant compared to the reduced repulsive interactions. Here, we see that the area ratio between dimer vacancy lines and atom vacancy lines is roughly 3:1, indicating that (2×1) structures are favored over (3×2) at ~0.6 ML of I.
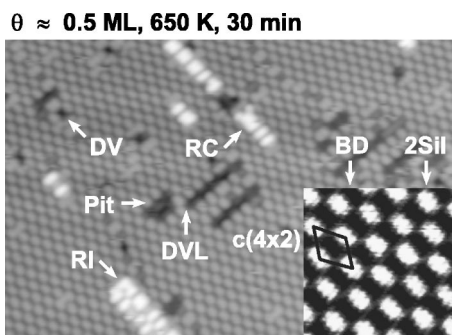
θ ≈ 0.5 ML, 650 K, 30 min

FIG. 6. Representative filled-state image $(-2\,\text{V}, 120\,\text{pA})$ of a surface with initial and final coverages of ~0.6 and ~0.5 ML (30 × 20 nm^2). The $c(4 \times 2)$ structure forms when alternate dimers are bare along and across the dimer row, as emphasized in the inset $(-2\,\text{V}, 120\,\text{pA})$ where bright features are Si dimers with two I atoms (2SiI) and dark ones are I-free dimers.

It is observed in large scanning areas $(200 \times 200\,\text{nm}^2)$ that one or both ends of atom vacancy lines are terminated by two-dimer-wide pits, as for the atom vacancy line pair in the lower left of Fig. 5(a). In contrast, there is no pit termination for the atom vacancy lines at higher I coverage, Fig. 4(a). Again, the changes are due to a decrease in the mean steric repulsive interactions at lower coverage. Previous studies of Cl-induced atom vacancy line formation showed that at least one end of the atom vacancy line was usually terminated with a two-dimer-wide pit. There is significant stress associated with the phase shift between the terrace dimer rows and the central dimer row of the atom vacancy line structure [the interface between (3×2) and (2×1) regions] and the two-dimer-wide pit provides a region to relax this stress.[3] Figure 4(a) shows that this termination is not necessary to stabilize the out-of-phase regions at ~0.8 ML because the stress is offset by the strong steric repulsions between I atoms. If the coverage is reduced to ~0.6 ML, Fig. 5, the reduced repulsive interactions are insufficient to offset the stress and the termination by two-dimer-wide pits becomes necessary.

Figure 6 is representative of a surface with a final coverage of ~0.5 ML (initial coverage ~0.6 ML). Alternate dimers are bare along and across the dimer row in extended areas, including on regrowth islands and in pits. The $c(4 \times 2)$ reconstruction is clear in the inset where the bright features are Si dimers with two I atoms, 2SiI, and the dark ones are bare dimers. The regrowth features were up to five dimers in width. Most of the pits are 1 - 4 dimers in width. In contrast to the surfaces at ~0.8 and ~0.6 ML, atom vacancy lines were rare at ~0.5 ML and below.

Since the mean steric repulsive interactions depend on the I coverage, we reasoned that the competition between dimer vacancy lines and atom vacancy lines could be controlled. To test this and to determine the transition coverage for I-Si(100), we reexposed the surface of Fig. 6 to reach ~0.6 ML and then annealed for 30 min at ~575 K to facilitate structural changes without I depletion. Imaging showed the reappearance of atom vacancy line structures. Annealing again for 30 min at 650 K decreased the I coverage to ~0.5 ML, the atom vacancy lines converted to dimer vacancy lines, and the area of dimer vacancy lines increased. We conclude that the transition between atom vacancy lines and dimer vacancy lines is between 0.5 and 0.6 ML. The fact that the transition coverage is lower than that for Br is consistent with the scaling of steric repulsive interactions because the transition is mainly determined by competition between steric repulsions and strain associated with (3×2)-(2×1) phase shifts.

IV. CONCLUSIONS

The adsorption of halogens on Si(100)-(2×1) alters the clean-surface dimer-dimer interactions and introduces adsorbate-adsorbate interactions that have important consequences for the equilibrium surface morphologies. These repulsive interactions increase in strength from Cl to Br to I. They cause surface roughening, and the patterns that are produced are sensitive to the magnitude of the interaction, with crossover from vacancy elongation along dimer row direction for Cl and Br to vacancy extension across dimer rows for I. Reducing the concentration from near saturation decreases the mean repulsive interaction, resulting in a transition from vacancies that elongate across the dimer row to those that elongate along the row. The atom vacancy lines dominate at ~0.8 ML, they coexist with dimer vacancy lines for ~0.6-0.7 ML, and dimer vacancy lines dominate below ~0.5 ML. It will remain for future work to determine the patterns for a surface with mixed adsorbates.

[1] K. S. Nakayama, E. Graugnard, and J. H. Weaver, Phys. Rev. Lett. **88**, 125508 (2002).

[2] C. F. Herrmann, D. Chen, and J. J. Boland, Phys. Rev. Lett. **89**, 096102 (2002).

[3] G. J. Xu, E. Graugnard, V. Petrova, K. S. Nakayama, and J. H. Weaver, Phys. Rev. B **67**, 125320 (2003).

[4] G. J. Xu, K. S. Nakayama, B. R. Trenhaile, C. M. Aldao, and J. H. Weaver, Phys. Rev. B **67**, 125321 (2003).

[5] G. J. Xu, E. Graugnard, B. R. Trenhaile, K. S. Nakayama, and J. H. Weaver, Phys. Rev. B **68**, 075301 (2003).

[6] C. M. Aldao, S. E. Guidoni, G. J. Xu, K. S. Nakayama, and J. H. Weaver, Surf. Sci. **551**, 143 (2004).

[7] C. M. Aldao and J. H. Weaver, Prog. Surf. Sci. **68**, 189 (2001).

[8] G. J. Xu, S. V. Khare, K. S. Nakayama, C. M. Aldao, and J. H. Weaver, Phys. Rev. B **68**, 235318 (2003).

[9] G. A. de Wijs and A. Selloni, Phys. Rev. B **64**, 041402(R) (2001).

[10] B. R. Trenhaile, V. N. Antonov, G. J. Xu, K. S. Nakayama, and J. H. Weaver, Surf. Sci. Lett. (to be published).

[11] de Wijs *et al.* (Ref. 12) reported that Cl adsorption on the dangling bonds of the terrace is favored by 1.9 eV relative to adsorption at sites within a single dimer vacancy. I adsorption shows an analogous preference for terrace sites.

[12] G. A. de Wijs, A. De Vita, and A. Selloni, Phys. Rev. B **57**, 10 021 (1998).

[13] A. Li, F. Liu, and M. G. Lagally, Phys. Rev. Lett. **85**, 1922 (2000).

[14] H. J. W. Zandvliet, Rev. Mod. Phys. **72**, 593 (2000).

[15] Y. Wei, L. Li, and I. S. T. Tsong, Appl. Phys. Lett. **66**, 1818 (1995).

[16] K. Wurm, R. Kliese, Y. Hong, B. Röttger, H. Neddermeyer, and I. S. T. Tsong, Phys. Rev. B **50**, 1567 (1994).

[17] R. J. Hamers, U. K. Köhler, and J. E. Demuth, Ultramicroscopy **31**, 10 (1989).

[18] Y.-W. Mo, B. S. Swartzentruber, R. Kariotis, M. B. Webb, and M. G. Lagally, Phys. Rev. Lett. **63**, 2393 (1989).

[19] G. Kresse and J. Hafner, Phys. Rev. B **47**, R558 (1993).

[20] G. Kresse, Ph.D. thesis, Technische Universität Wien, 1993.

[21] G. Kresse and J. Furthmüller, Comput. Mater. Sci. **6**, 15 (1996).

[22] G. Kresse and J. Furthmüller, Phys. Rev. B **54**, 11 169 (1996).

[23] D. Vanderbilt, Phys. Rev. B **41**, 7892 (1990).

[24] G. Kresse and J. Hafner, J. Phys.: Condens. Matter **6**, 8245 (1994).

[25] H. J. Monkhorst and J. D. Pack, Phys. Rev. B **13**, 5188 (1976).

[26] Comparison of the energies associated with creation of a dimer vacancy line and a vacancy line defect of odd finite length gives the same result. Odd lengths are favored for dimer vacancy lines (Ref. 3) but this is not necessarily the case for vacancy line defects.

[27] J. Tersoff, Phys. Rev. B **45**, R8833 (1992).

[28] X. Chen, F. Wu, Z. Zhang, and M. G. Lagally, Phys. Rev. Lett. **73**, 850 (1994).

[29] P. Bedrossian and T. Klitsner, Phys. Rev. Lett. **68**, 646 (1992).

[30] H. Feil, H. J. W. Zandvliet, M.-H. Tsai, J. D. Dow, and I. S. T. Tsong, Phys. Rev. Lett. **69**, 3076 (1992).

[31] H. J. W. Zandvliet, H. K. Louwsma, P. E. Hegeman, and B. Poelsema, Phys. Rev. Lett. **75**, 3890 (1995).

[32] The results reported here are not induced by Ni contamination since the latter are manifest as (1) line scan profiles that are deeper than one atomic layer (Ref. 31), (2) vacancies that persist or increase in number with further flashing to 1475 K, and (3) structures that are usually of the form DV-DV-dimer-DV in a row (Ref. 33). Secondary ion mass spectroscopy and x-ray photoelectron spectroscopy of our samples detected no Ni. Finally, vacancy line defects were produced by I near saturation but atom vacancy lines and dimer vacancy lines were produced at low coverage.

[33] V. A. Ukraintsev and J. T. Yates, Jr., Surf. Sci. **346**, 31 (1996).

[34] H. J. W. Zandvliet, Surf. Sci. **377**, 1 (1997).

[35] P. Zeppenfeld, M. Krzyzowski, C. Romainczyk, G. Comsa, and M. G. Lagally, Phys. Rev. Lett. **72**, 2737 (1994).

[36] A. R. Smith, F. K. Men, K. J. Chao, Z. Zhang, and C. K. Shih, J. Vac. Sci. Technol. B **14**, 909 (1996).

[37] P. C. Weakliem, Z. Zhang, and H. Metiu, Surf. Sci. **336**, 303 (1995).

[38] M. H. Tsai, Y. S. Tsai, C. S. Chang, Y. Wei, and I. S. T. Tsong, Phys. Rev. B **56**, 7435 (1997).

[39] D. J. Chadi, Phys. Rev. Lett. **59**, 1691 (1987).